Rheology and Morphology of Phase-Separating Polymer Blends

Z. L. Zhang,[†] H. D. Zhang,[†] Y. L. Yang,*[,†] I. Vinckier,[‡] and H. M. Laun[§]

Department of Macromolecular Science, Open Lab of Macromolecular Engineering, SEDC, Fudan University, Shanghai 200433, China; Chemical Engineering Department, K.U. Leuven, B-3001 Leuven, Belgium; and Polymer Physics Department, BASF Aktiengesellschaft, 67056 Ludwigshafen, Germany

Received June 1, 2000; Revised Manuscript Received September 5, 2000

ABSTRACT: Simulations of phase separation under oscillatory shear flow have been performed based on the time-dependent Ginzburg−Landau (TDGL) equation. To calculate the stress tensor, the expression proposed by Kawasaki was used. The results of the simulations have been confronted directly with experimental results on a LCST blend of PαMSAN/PMMA to evaluate the potential of the simulations. The effect of quench depth, shear amplitude, and shear frequency on the morphology development as well as on the corresponding rheological properties has been investigated. The results show that the characteristic rheological behavior of phase-separating systems can be attributed to the interfacial relaxation, which is changing during the process of phase separation. The strength of the concentration fluctuations and the interfacial volume fraction are key factors determining the contribution of interfacial relaxation to the global rheological behavior of the blend. In the low frequency range, the oscillatory shear cannot affect the critical point, but it can accelerate the coagulation and growth of the blend morphology. The simulations qualitatively agree with the experimental findings.

I. Introduction

The rheology of polymer blends has received a lot of attention because of its technological importance in polymer processing as well as for theoretical reasons, since a lot of physical problems still need to be clarified. These studies can be classified into three groups: studies dealing with the rheology of polymer mixtures in respectively homogeneous, phase-separated and transition regimes. Research on homogeneous blends is focused mainly on the concentration dependence of viscosity and linear dynamic properties.[1−3] These rheological properties can be determined by the simple Irving relation.[4] Mertsch and Wolf[5] modified this relation by taking into account the differences in molecular shape of the components, an approach which is confirmed experimentally by Vlassopoulos et al.[6] and Kapnistos et al.[7] It is important to note that the time−temperature superposition (TTS) applied well when polymer blends were in the homogeneous state far from the transition temperature and there is no obvious dynamic asymmetry of the components.[6−13] The characteristic power law of storage moduli $G' \sim \omega^2$ and loss moduli $G'' \sim \omega$ were observed at low angular frequency ω.

The rheological behavior of phase-separated polymer blends has also been studied extensively, both experimentally and theoretically.[14−16] In this regime, the polymer blends show pronounced elastic properties, very long relaxation times and a failure of the TTS. The linear viscoelastic behavior of polymer blends with a droplet−matrix structure can be described quantitatively[17] by the emulsion model proposed by Palierne.[18] Additionally, this model has been widely used to obtain either the interfacial tension or structural information (domain size and distribution) from linear dynamic measurements.[19,20]

Polymer blends in the transitional regime also exhibit abnormal rheological behavior.[6−12] Complex changes in the linear viscoelastic properties were observed when polymer blends of a given composition were heated (for LCST systems) or cooled (for UCST systems) from homogeneous regime to phase separation regime. Different observations are made for the time evolution of the dynamic moduli. The moduli can show a monotonic increase,[11] a monotonic decrease,[10,11] or both.[7,12] In the latter studies, the moduli increased in the early stage of phase separation; in the late stages of phase separation they decreased. Polios et al.[12] attribute the initial increase of the moduli to the formation of a highly interconnected network, and the subsequent decrease was considered to be the result of the loss of the interconnectivity due to breakup. In a study on phase separation in a PαMSAN/PMMA blend it was demonstrated that droplet−matrix formation results in an increase in moduli whereas during the coarsening of a co-continuous structure the moduli will decrease.[21]

Isothermal frequency sweep experiments showed that TTS fails for phase-separating systems. At low frequencies, the development of a shoulder in the G' curve could be observed. Ajji et al.[10] used the theoretical treatment of Fredrickson and Larson[22] to explain this phenomenon. In the work of Fredrickson and Larson, the mean-field theory has been employed to derive the concentration fluctuation contribution to the shear stress for near-critical polymer mixtures. Similar work has been done by Kapnistos et al.[7,13] and Vlassopoulos et al.[6] All their results revealed that this rheological abnormality should be attributed to the enhanced concentration fluctuations in the transitional regime. Kapnistos et al.[7] quantified this effect and showed how the full phase diagram (both binodal and spinodal curves) can be derived from rheological measurements.

However, there are still unsolved problems in the area of theoretical modeling of the interrelationship between

* To whom correspondence should be addressed. E-mail: ylyang@srcap.stc.sh.cn.
[†] Fudan University.
[‡] K.U. Leuven.
[§] BASF Aktiengesellschaft.

10.1021/ma000968f CCC: $20.00
Published on Web 01/26/2001

the rheological behavior and the morphology evolution during the process of phase separation. The theoretical model of Fredrickson and Larson[22] can only explain the rheological behavior in homogeneous state or near the critical point. On the other hand, the emulsion model of Palierne[18] attributes the abnormal rheological behavior to the interfacial relaxation of droplet domains. This model is however limited to rather dilute droplet/matrix blends. A general model for the rheological behavior of polymer blends, without constraints on the degree of miscibility or on the type of morphology, is still lacking.

Another remaining problem is the coupling between phase separation and shear. The effects of shear on phase separation of polymer blends are generally very complex. Hindawi,[23] Katsaros,[24] and Fernandez[25] found that shear can induce both mixing and demixing, depending on composition, temperature and shear rate or frequency. Larson[26] has done systematic research on mixing, demixing and other transitions induced by shear. Theoretical[23,27,28] and experimental studies[29] to understand this complex problem more or less agree that shear will not affect the critical temperature when the shear rate or frequency is low enough. This is also true for oscillatory shear in which the average strain is zero. The resulting morphology, however, can be affected by shear flow, even at low rate or frequency. Qiu et al.[30] found that oscillatory shear can induce different regular morphologies depending on quench depth. On one hand, the growth of droplets will be suppressed: if the radius exceeds some critical value the droplets tend to break up due to shear. The predicted critical radius and shear rate depend on whether the chain stretching effect and the hydrodynamic interaction were taken into account.[31,32] On the other hand, the coagulation and growth can also be accelerated by shear.[28,29] Although the shear will not affect the orientation of molecular chains when the shear rate or frequency is low, it is still necessary and interesting to study the coupling between shear and morphology evolution as well as the effects on the corresponding rheological response.

In the present paper, we intend to simulate the morphology evolution and the corresponding rheology of a phase-separating blend under oscillatory shear. The simulations are based on the time-dependent Ginzburg−Landau (TDGL) equation. The aim of present work is not to produce more simulation results but rather to confront the simulations directly with experimental work to evaluate the potential of the simulations. Additionally, a physical explanation will be proposed for the observed evolution of the rheological properties during phase separation, based on the underlying morphological processes. The paper is organized as follows: the theoretical model and simulation scheme is presented in section II. Subsequently, the materials and methods of the experimental study are described in section III. A systematic overview of the simulation results is shown in section IV. This section includes the discussion of the effect of phase-separating temperature and shear amplitude and a qualitative comparison with experimental results is made. Finally the main conclusions are summarized.

II. Theoretical Model and Simulation Scheme

In this work, we only consider low shear rates or frequencies, which do not induce any chain stretching.[31] Under these conditions, the time evolution of order parameter $\psi(\mathbf{r},t)$ is governed by the following modified time-dependent Ginzburg−Landau TDGL equation[30]

$$\frac{\partial\psi(\mathbf{r},t)}{\partial t} = -\mathbf{v}(\mathbf{r})\cdot\nabla\psi(\mathbf{r},t) = \nabla\left[M(\psi)\nabla\frac{\delta H\{\psi\}}{\delta\psi}\right] \quad (1)$$

where $\psi(\mathbf{r},t)$ is defined as $\phi_A(\mathbf{r}) - \phi_B(\mathbf{r})$, i.e., the difference between the local volume fractions of component A and B. $\mathbf{v}(\mathbf{r})$ represents the flow field. $M(\psi)$ is the mobility and depends on the order parameter. This dependency is usually expressed as $M(\psi) = M_0(1 - \alpha\psi^2)$ with α being a coefficient between 0 (bulk diffusion) and 1 (diffusion only in the vicinity of the interface).[32] $H\{\psi\}$ is the free energy functional of the order parameter field $\psi(\mathbf{r},t)$ for the system, expressed per unit of the thermal energy k_BT

$$H\{\psi\} = \int \mathrm{d}r \left[F(\psi) + \frac{1}{2}D(\nabla\psi)^2\right] \quad (2)$$

where $F(\psi)$ is a function of ψ with two local minima, whose explicit form will be given later. The term $D(\nabla\psi)^2$ represents the interfacial free energy derived from the spatial composition inhomogeneity. D is defined as $b^2/(9(1 - \psi^2))$ where b is the Kuhn statistical segment length.[32] Substituting eq 2 into eq 1 yields

$$\frac{\partial\psi(r,t)}{\partial t} = -\mathbf{v}(\mathbf{r})\cdot\nabla\psi(\mathbf{r},t) + \nabla\left[M(\psi)\nabla\left(\frac{\mathrm{d}F(\psi)}{\mathrm{d}\psi} - D\nabla^2\psi\right)\right] \quad (3)$$

The flow field $\mathbf{v}(\mathbf{r})$ is simply the externally imposed oscillatory shear flow

$$\mathbf{v}(\mathbf{r}) = (y\Gamma\omega\cos\omega t, 0, 0) \quad (4)$$

where Γ is the amplitude of the oscillatory shear strain and ω the angular frequency.

Equation 3 is simulated by using cell dynamical scheme (CDS) proposed by Onoo and Puri.[34,35] This approach has been proven to be adequate for investigation of the morphology evolution during (the late stages of) phase separation. For simplicity reasons, only two-dimensional simulations have been performed. In the CDS approach, a two-dimensional system is discretized on a $L\times L$ square lattice of cell size a_0, and the order parameter for each cell is defined as $\psi(\mathbf{n},t)$, where $\mathbf{n} = (n_x,n_y)$ is the lattice position and n_x and n_y are integers between 1 and L. The Laplacian in CDS is approximated by

$$\nabla^2\psi(\mathbf{n}) = \frac{1}{a_0^2}(\langle\langle\psi(\mathbf{n})\rangle\rangle - \psi(\mathbf{n})) \quad (5)$$

where $\langle\langle\psi(\mathbf{n})\rangle\rangle$ represents the following summation of $\psi(\mathbf{n})$ for the nearest neighbors (n.), the next-nearest neighbors (n.n.), and the next-next-nearest neighbors (n.n.n.)

$$\langle\langle\psi(\mathbf{n})\rangle\rangle = B_1\sum_{\mathbf{n}=\mathrm{n}}\psi(\mathbf{n}) + B_2\sum_{\mathbf{n}=\mathrm{n.n.}}\psi(\mathbf{n}) + B_3\sum_{\mathbf{n}=\mathrm{n.n.n.}}\psi(\mathbf{n}) \quad (6)$$

with B_1, B_2, and B_3 being $^1/_6$, $^1/_{12}$, and 0 for a two-dimensional system.

Often the Ginzburg−Landau form of the mixing free energy functional $F(\psi)$ is used, which is a power series expansion of $\psi(\mathbf{r})$: $-(\tau/2)\,\psi^2 + (g/4)\psi^4$ where τ and g are positive coefficients. That is a function of ψ with

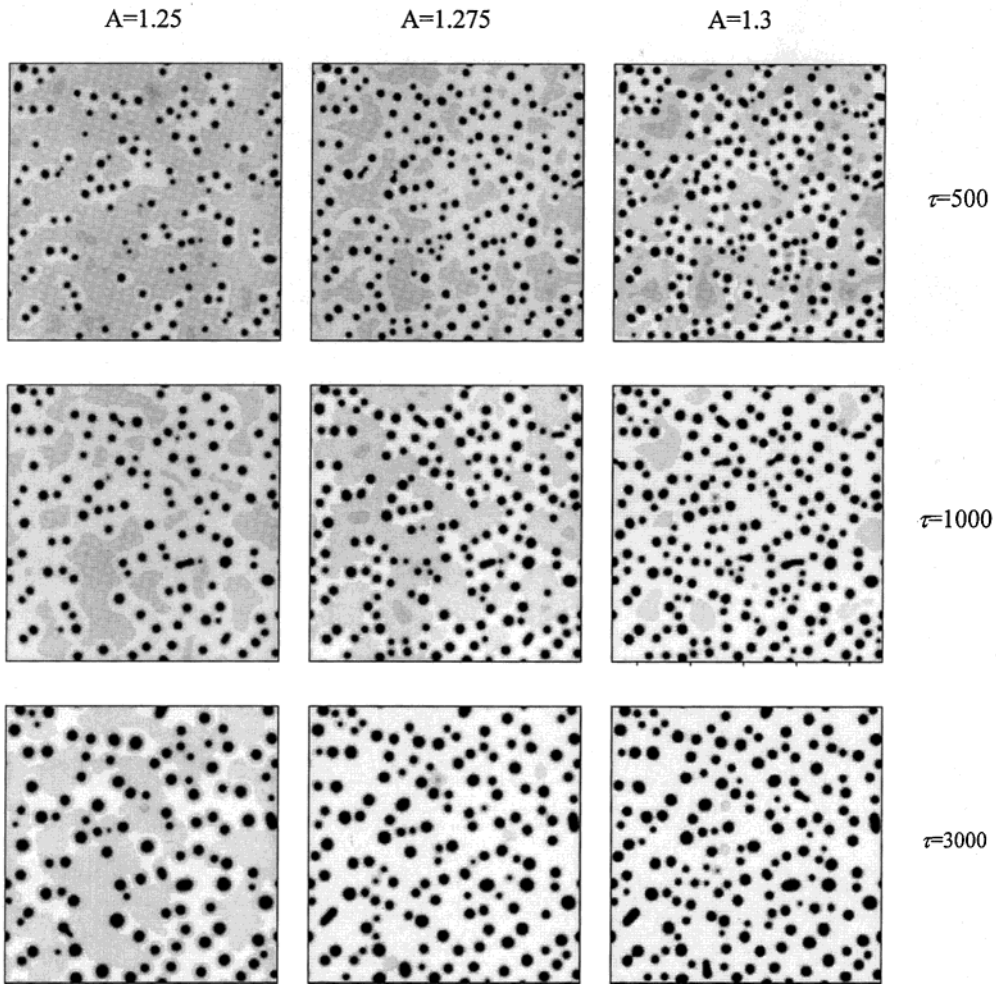

Figure 1. Effect of the quench depth A on the morphology evolution of a 20/80 blend ($\phi = 0.2$).

two local minima as mentioned previously. In the CDS approach, $dF/d\psi$ is chosen as $-A \tanh \psi + \psi$[34,35] where A is a phenomenological parameter greater than 1. This form possess the same features as Ginzburg−Landau form when $A > 1$. Furthermore, it has better numerical stability compared with the Ginzburg−Landau form. The greater A is, the more incompatible the system becomes. Actually, this parameter is proportional to the temperature for LCST systems and inversely proportional to the temperature for UCST systems. In other words, quench depth is controlled by this parameter. Roths et al.[36] use an even different expression for $dF/d\psi$, suited for strongly incompatible polymer pairs. However, as the equation for $dF/d\psi$ from the CDS approach is more general, only this expression will be used in the further discussion.

Equation 3 can be rewritten in a dimensionless form with a_0 and $\tau_0 = a_0^2/M_0$ as the unit of respectively length and time scale

$$\frac{\partial \psi}{\partial \tau} = -\Gamma\Omega \cos \Omega\tau \cdot \tilde{y}\frac{\partial \psi}{\partial \tilde{x}} + \nabla\left[\frac{M(\psi)}{M_0}\nabla(-A \tanh \psi + \psi - \tilde{D}\nabla^2\psi)\right] \quad (7)$$

where $\tau = t/\tau_0$, $\Omega = \omega\tau_0$, $\tilde{y} = y/a_0$, $\tilde{x} = x/a_0$, and $\tilde{D} = D/a_0^2$. In the CDS approach, $\tilde{D}$ was usually fixed at 0.5.

Our simulation was carried out on a two-dimensional square lattice of $L \times L = 256 \times 256$. We have chosen the x-axis as the flow direction, while the y-axis is the velocity gradient direction. We set $y = 0$ at $n_y = 128$.

For the x direction, a shear periodic boundary condition proposed by Ohta et al.[37] has been used. With the strain γ, this boundary condition can be written as

$$\psi(n_x, n_y, \tau) = \psi(n_x + N_x L + \gamma(\tau) N_y L,\ n_y + N_y L) \quad (8)$$

where N_x, N_y are arbitrary integers.

For phase-separating systems the total stress consists of two parts: the contribution of chain relaxation and that of interfacial relaxation. The total stress tensor of the system should be written as

$$\sigma_{\alpha\beta}^{T} = \sigma_{\alpha\beta}^{Int} + \sigma_{\alpha\beta}^{Rouse} + \eta(\kappa_{\alpha\beta} + \kappa_{\beta\alpha}) + p\delta_{\alpha\beta} \quad (9)$$

where $\sigma_{\alpha\beta}^{Int}$ is the stress contribution due to the interface, p is the pressure, $\sigma_{\alpha\beta}^{Rouse}$ is the Rouse stress tensor due to chain relaxation, η is the viscosity of the system, and $\kappa_{\alpha\beta}$ is the $\alpha\beta$-component of the velocity gradient. The Rouse contribution is independent of the morphology, and consequently, it should not be responsible for the rheological abnormality in phase-separating systems. We should mention that it is also true for the entangled systems due to the fact that the relaxation time of domain deformation and growth should be much slower than the terminal chain relaxation time at given temperature. Therefore, we only focus on the interfacial stress contribution in our simulation.

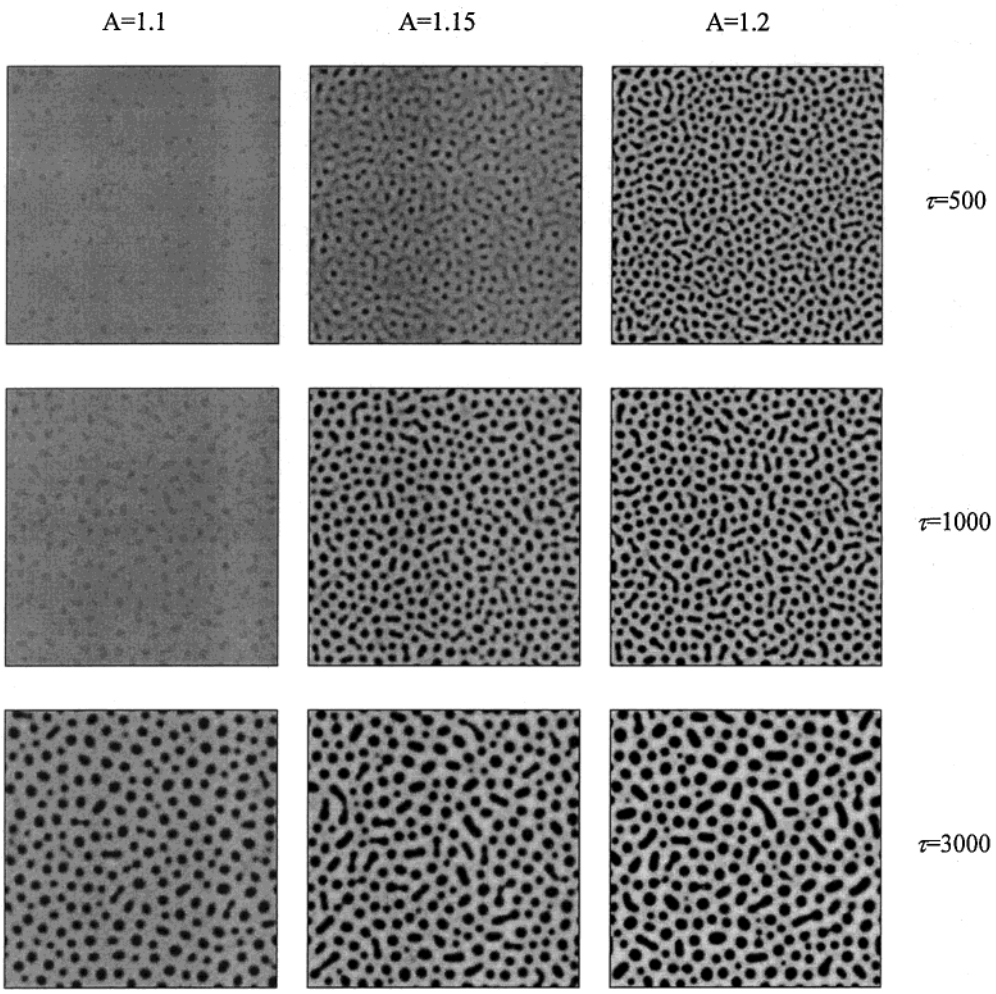

Figure 2. Effect of the quench depth A on the morphology evolution of a 40/60 blend ($\phi = 0.4$).

The formula of stress tensor from the interface relaxation has been derived by Kawasaki.[38] It reads

$$\sigma_{\alpha\beta} = -k_B T \frac{\tilde{D}}{V} \int \mathrm{d}r \, \frac{\partial \psi}{\partial r_a} \frac{\partial \psi}{\partial_{r\beta}} \quad (\alpha, \beta = x, y) \qquad (10)$$

Using the Fourier component $\psi(q,\tau)$, the stress tensor is then calculated as follows

$$\sigma_{\alpha\beta} = -\frac{\tilde{D}}{L^4} \sum q_a q_\beta |\psi(\boldsymbol{q},\tau)|^2 \quad (\alpha, \beta = x, y) \qquad (11)$$

where the stress is expressed in units of $k_B T$.

The storage modulus G' and the loss modulus G'' were obtained by a linear fit of the simulated stress−strain curve. The fit equation is written as

$$\sigma_{xy} = \Gamma[G' \sin(\Omega\tau) + G'' \cos(\Omega\tau)] \qquad (12)$$

The expression of Kawasaki[38] (eq 10) indicates that the contribution of interfacial relaxation is mainly determined by two factors: the strength of concentration fluctuations and the interfacial area per unit volume. In fact, all the simulation results can be explained by the changes of these two factors during phase separation. Another important point that should be noted is the universality of stress tensor expression proposed by Kawasaki. From a physical point of view, his treatment is consistent with that of Fredrickson and Larson.[22] The approach of Kawasaki allows, however, for a relatively easy calculation of the stress tensor, even in the late stages of phase separation. In the late stage of phase separation, the rheological behavior can alternatively be calculated with an emulsion model.[18] Such models are limited to polymer blends with a droplet−matrix structure. The emulsion models calculate the extra stress due to relaxation of the droplet surface, a stress contribution that is included in the expression by Kawasaki. Compared with the emulsion model, the expression of the stress tensor proposed by Kawasaki can more easily deal with a concentration dependence of surface tension, and it can be extended to the case of bicontinuous phase separation.

Finally, it should be mentioned that the above model is applicable only for processes on spatial scales longer than the gyration radius of the polymers and for blends in which the two components have the same viscoelastic properties.[30]

III. Materials and Methods

Experimental Study. Most of the experimental studies in the literature[6−12] treat the phase separation in mixtures of two polymers with a large difference in T_g, such as polystyrene (PS) and polyvinyl methyl ether (PVME). As the above model is applicable only for blends with components that have the same viscoelastic properties, these existing experimental results cannot be used to assess the model predictions. Therefore, a pair of rheologically similar polymers has been selected here for an experimental study. A study within the frame of IUPAC Working Party IV.2.1. "Structure and properties of commercial polymers" shows that PαMSAN (Luran KR

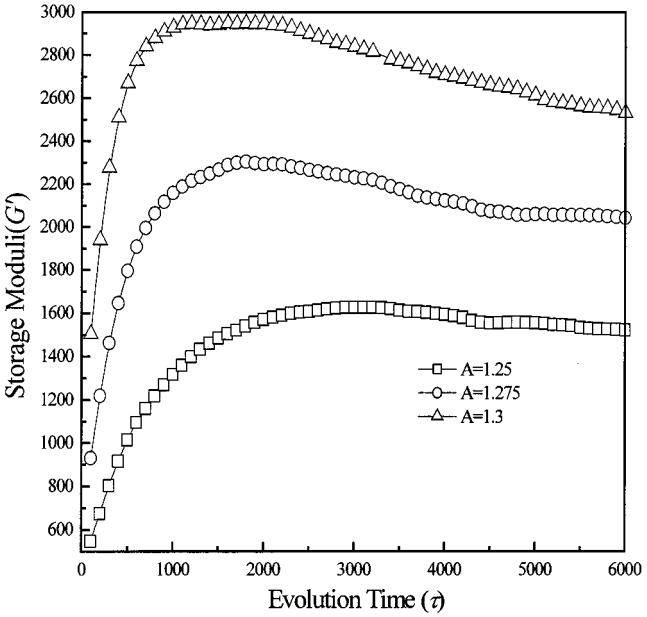

Figure 3. Simulation result of G' changing with phase separation (composition 20/80, $\Gamma = 5\%$, $\Omega = 0.01$).

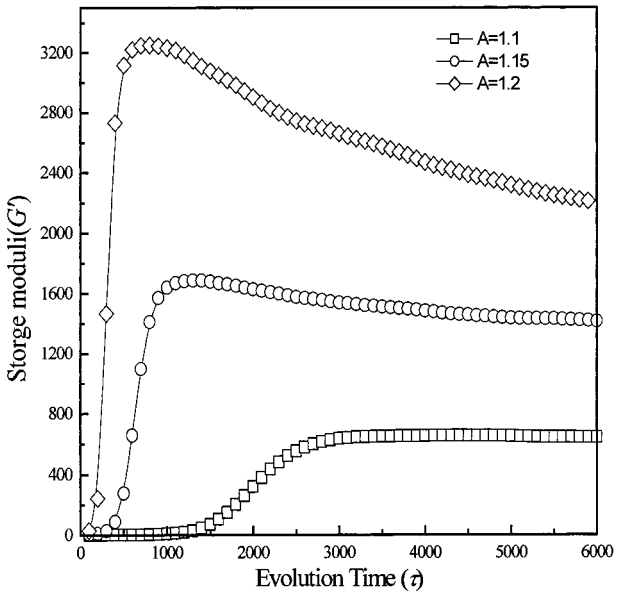

Figure 4. Simulation result of G' changing with phase separation (composition 40/60, $\Gamma = 5\%$, $\Omega = 0.01$).

2556 from BASF) and PMMA (Lucryl G77 from BASF) can meet this requirement.[39] Lucryl G77 is a copolymer of 95% methyl methacrylate and 5% methyl acrylate. Its weight-average molecular weight determined by light scattering is $M_w = 88\,000$. GPC (PS-calibration) gives $M_w/M_n = 2.1$. Luran KR 2556 is a copolymer of 70% α-methylstyrene and 30% acrylonitrile. Its weight-average molecular weight determined by light scattering is $M_w = 82\,000$. GPC (PS calibration) gives $M_w/M_n = 2.4$. Mixtures of these polymers show LCST behavior, and their linear dynamic behavior at 210 °C is very similar: the only difference is the relaxation times of PMMA being a factor 1.64 shorter than those of PαMSAN.[39] The temperature dependencies of the rheological properties of the two melts are almost identical in the range of 150 to 230 °C; the T_g values are 124 (PαMSAN) and 109 °C (PMMA).[39]

Blends of 15/85 wt % PMMA/PαMSAN and 40/60 wt % PMMA/PαMSAN have been selected for this study. The blend preparation technique is described elsewhere.[39] The cloud points of these mixtures are 190 and 175 °C, respectively. A previous study has shown that at 220 °C the 15/85 blend phase

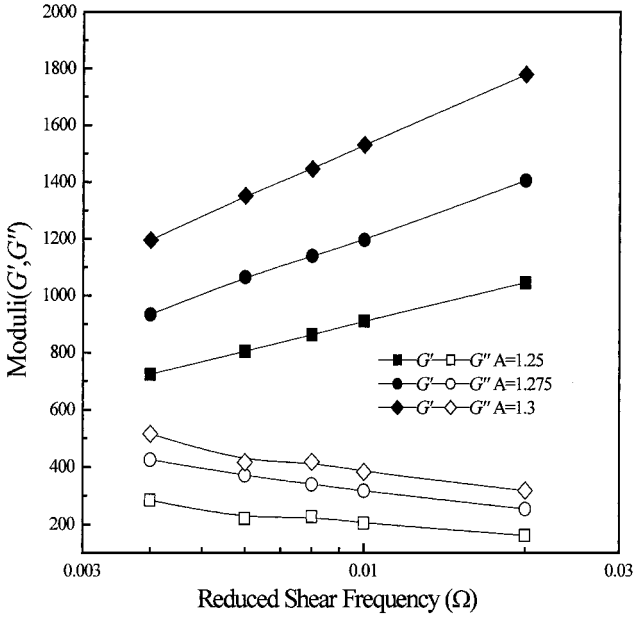

Figure 5. Simulation results of G' and G'' in frequency sweep measurement ($\tau = 3000$, composition 20/80, $\Gamma = 5\%$).

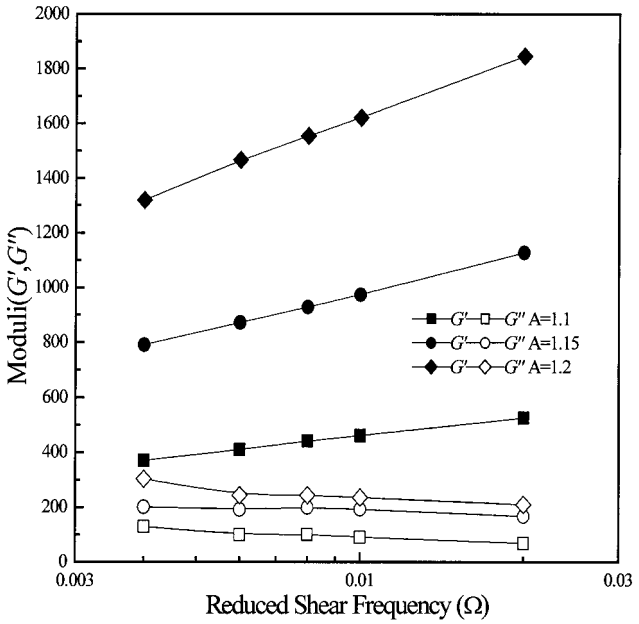

Figure 6. Simulation results of G' and G'' in frequency sweep measurement ($\tau = 3000$, composition 40/60, $\Gamma = 5\%$).

separates by a nucleation and growth mechanism and the 40/60 mixtures show spinodal decomposition.[21] To study phase separation under oscillatory flow, homogeneously mixed samples were inserted in a rheometer that was preheated at 220 °C. An oscillatory strain was applied during the subsequent phase-separation process and the corresponding stress response was measured. Morphological investigations were performed by either TEM (15/85 blend) or light microscopy (40/60) on samples that were quenched in the rheometer. The experimental findings will be compared with the simulation results to evaluate the potential of the simulations. At this point, we will only concentrate on a qualitative comparison.

Simulations. The simulations will be used to show how the phase separation proceeds and how quench depth, composition, shear amplitude, and evolution time affect the interfacial stress response. Different kinds of simulations have been preformed.

First, the effect of morphology on the rheological properties has been studied. Therefore, the phase separation process and

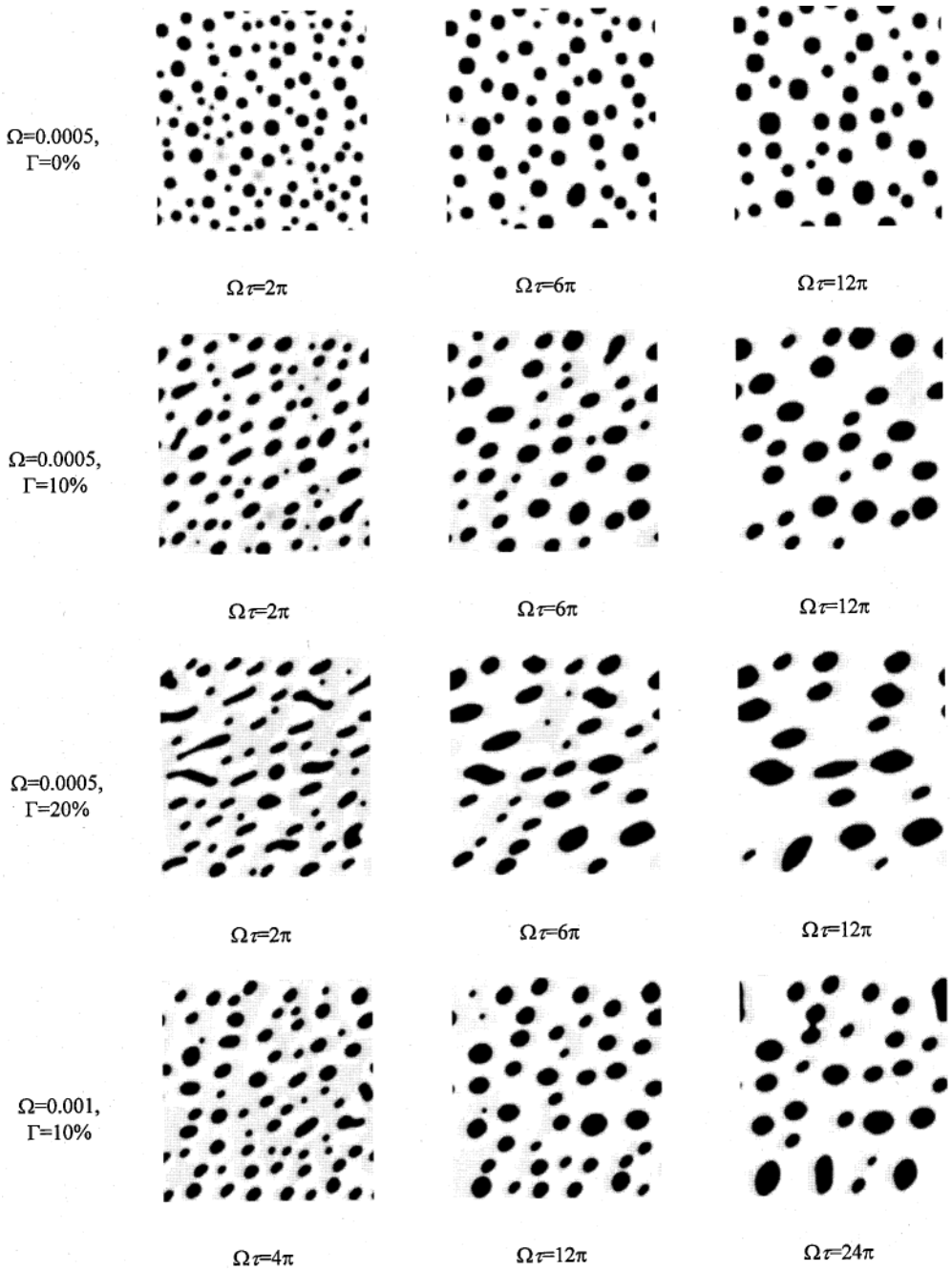

Figure 7. Effect of shear amplitude and frequency on the morphology evolution of polymer blend during phase separation under oscillatory shear ($A = 1.3$, composition 20/80).

the rheological measurement were decoupled. We carried out the simulation of the phase separation process under quiescent conditions during a particular time interval. The corresponding rheological response at that stage in the morphology evolution was obtained by a subsequent simulation of a shear measurement (strain amplitude = 5%, reduced frequency 0.01). To distinguish the two kinds of simulations, the former is called simulation of the phase separation and the latter is called the simulation of the rheological response. In this procedure, the possible effect that the rheological measurement (oscillatory flow) could have on the morphology evolution is not taken into account. If we additionally switched off the diffusion (by setting $M = 0$) in the simulation of rheological response (to acquire relatively stable stress-strain curves), only the storage modulus could be determined because the loss modulus is nearly zero under this simplification. If both the loss and the storage modulus were to be determined, e.g., to mimic the isothermal frequency sweep experiments, we performed a simulation of a frequency sweep in which we did not stop the diffusion in the simulation of the rheological response.

Second, simulations have been performed in which the coupling between the phase separation process and the oscillatory flow is no longer neglected. Phase separation was allowed to proceed under a particular shear amplitude and frequency during a particular time interval. Subsequently, a shear measurement was simulated in order to acquire corresponding rheological response. For the latter a strain amplitude of 5% and a reduced frequency of 0.01 were chosen. The results of the simulations are presented in a dimensionless form; only qualitative comparison with the experimental results will be made.

IV. Results and Discussion

The Effect of Quench Depth on Phase Separation under Quiescent Conditions. A previous study has shown that, depending on the temperature at which the phase separation is performed, different morphol-

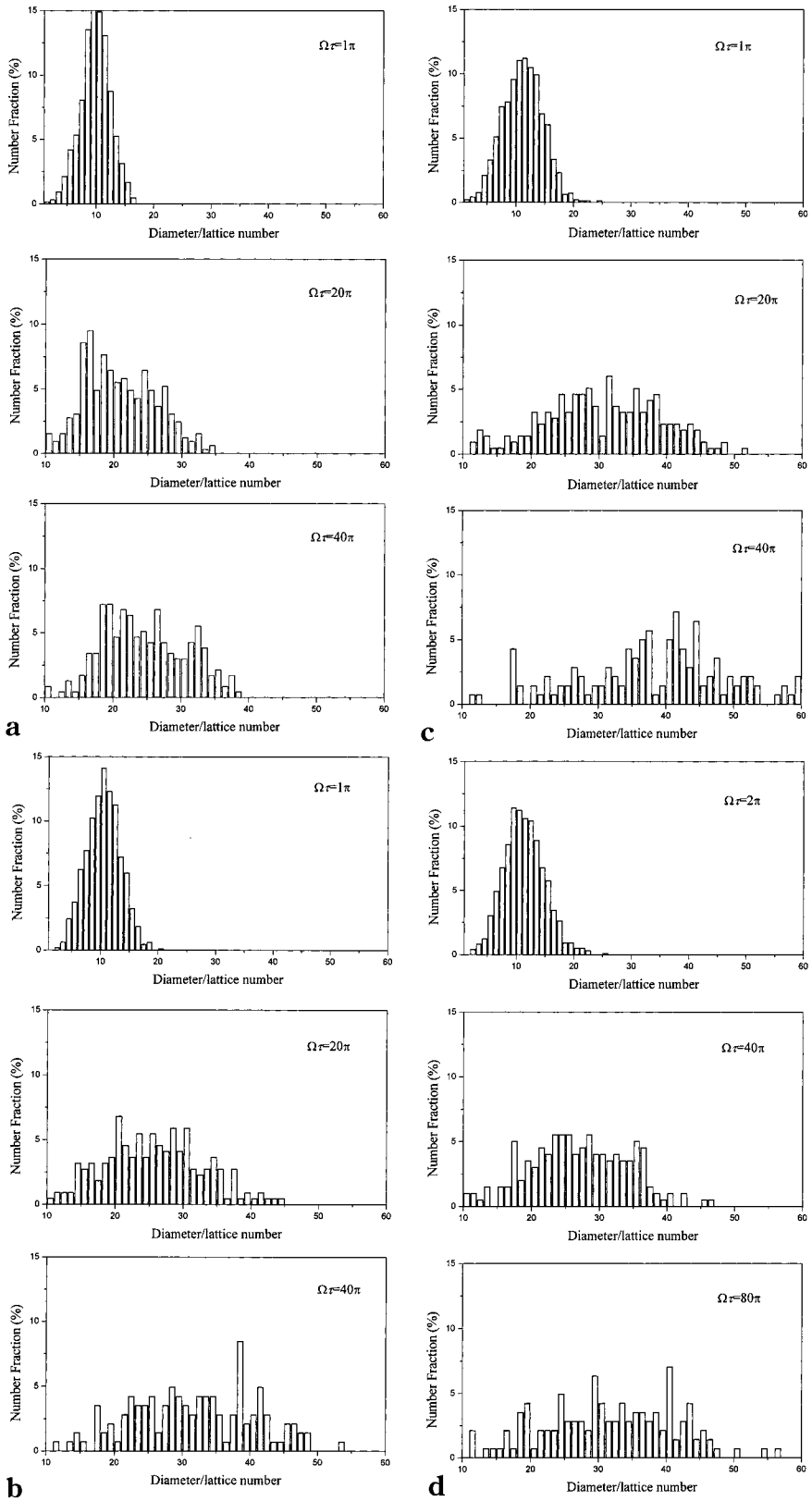

Figure 8. (a) Droplet size distributions of the morphologies displayed in Figure 7 (composition 20/80, $A = 1.3$, $\Gamma = 0\%$, $\Omega = 0.0005$). (b) Droplet size distributions of the morphologies displayed in Figure 7 (composition 20/80, $A = 1.3$, $\Gamma = 10\%$, $\Omega = 0.0005$). (c) Droplet size distributions of the morphologies displayed in Figure 7 (composition 20/80, $A = 1.3$, $\Gamma = 20\%$, $\Omega = 0.0005$). (d) Droplet size distributions of the morphologies displayed in Figure 7 (composition 20/80, $A = 1.3$, $\Gamma = 10\%$, $\Omega = 0.001$).

ogies can be formed,[40] eventually leading to a different rheological behavior. Therefore, the effect of quench depth will be determined by our simulations, in which the quench depth is controlled by the parameter A.

The morphology evolution resulting from phase separation under quiescent conditions is illustrated in Figures 1 and 2 for a composition of respectively 20/80 (droplet−matrix structure) and 40/60 (bicontinuous

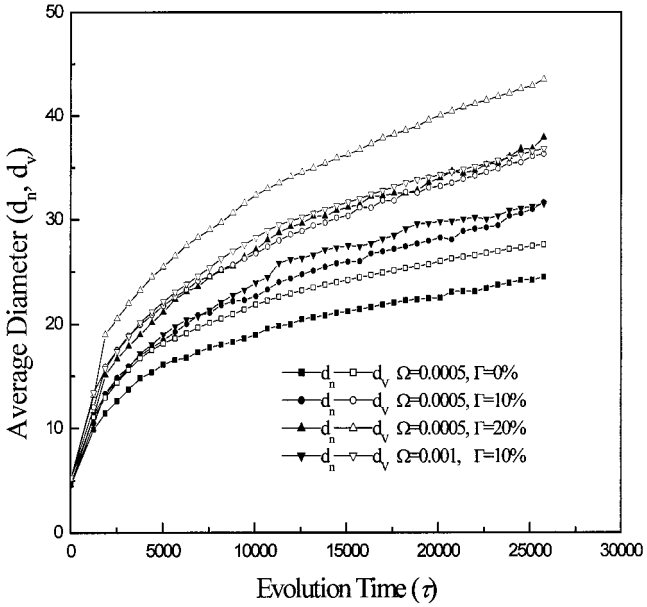

Figure 9. Evolution of the average droplet sizes (d_n and d_v) of polymer blend during phase separation under oscillatory shear ($A = 1.3$, composition 20/80).

structure). It can be seen that the strength of the concentration fluctuations clearly increases with quench depth. For the droplet−matrix system (Figure 1) the number of nuclei also increases with the quench depth.

How this is reflected in the rheological properties, or rather in the storage modulus, is illustrated in Figures 3 and 4. The coupling between phase separation and shear is not taken into account here. The storage modulus initially increases and subsequently decreases. This can be explained by considering the effects of concentration fluctuations and of the specific interfacial area. Initially, the storage modulus of the blend increases due to an increase in both the concentration fluctuations and the specific interfacial area. In droplet−matrix systems, it is mainly the increase in interfacial area (due to the increase in volume fraction of the disperse phase) which contributes to the initial stress increase, whereas the growth of concentration fluctuations plays the major role in co-continuous phase separation. After some time, the concentration fluctuations become saturated and the volume fraction of both phases remains constant. The interfacial area per unit volume will decrease from that point on due to interfacial tension driven coarsening (in co-continuous systems) or coalescence and Oswald ripening (in droplet−matrix systems), inducing a decrease of storage modulus. The G' peak was reached more rapidly for the more concentrated systems (compare Figures 3 and 4), which is reasonable considering that the coagulation and growth of domains is faster at higher concentrations.

However, one comment on droplet−matrix systems should be made. It can be deduced from the Palierne model[18] that an increase in droplet size gives rise to a decrease in G' only for intermediate frequencies. For very low frequencies, the interfacial contribution to the storage modulus is proportional to the droplet size. This behavior can be explained based on the deformability of the droplets. Small droplets have a higher specific interfacial area but are less deformable than larger ones, and therefore, the storage modulus of a coarse morphology is larger than for a finer morphology. Therefore, there is a frequency range at which an

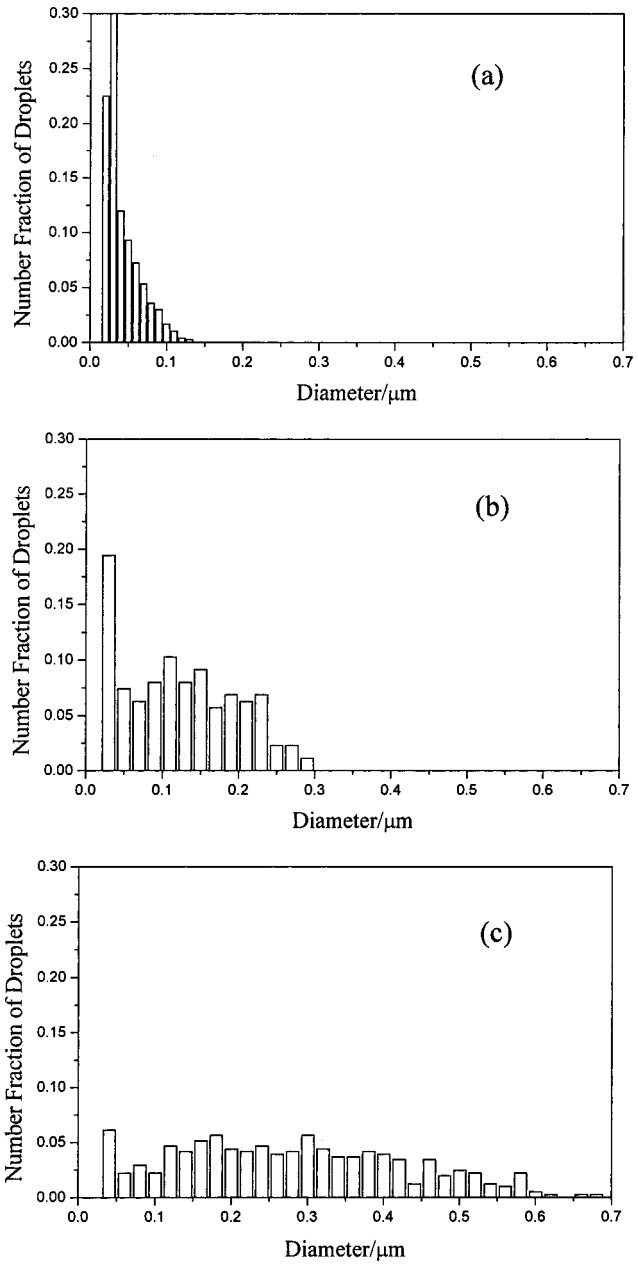

Figure 10. Apparent droplet size distribution (TEM) for 15/85 PMMA/PαMSAN. The sample was maintained under quiescent conditions at 220 °C for a certain period of time and subsequently subjected to a frequency sweep ($\omega = 100-0.01$ rad/s, $\gamma = 20\%$, duration = 60 min): (a) 7 min quiescent phase separation, (b) 37 min quiescent phase separation + frequency sweep, and (c) 307 min quiescent phase separation + frequency sweep.

increase in droplet size results in an increase in G'. This frequency range shifts to lower frequencies for larger droplets, because the relaxation time of the droplets is proportional to their size. If one looks at one particular frequency, just like in our simulations, one can observe an increase in G' and a subsequent decrease in G' until a plateau is reached (no contribution from the interface any more). Actually this phenomenon has been observed in Figure 3. The greater A is, the faster the phase separation is occurring. Consequently the G' peak will shift to smaller times just as observed in Figure 3.

As mentioned above, frequency sweeps in which we did not stop the diffusion in the simulation of rheological response were performed as well. In this case, we also

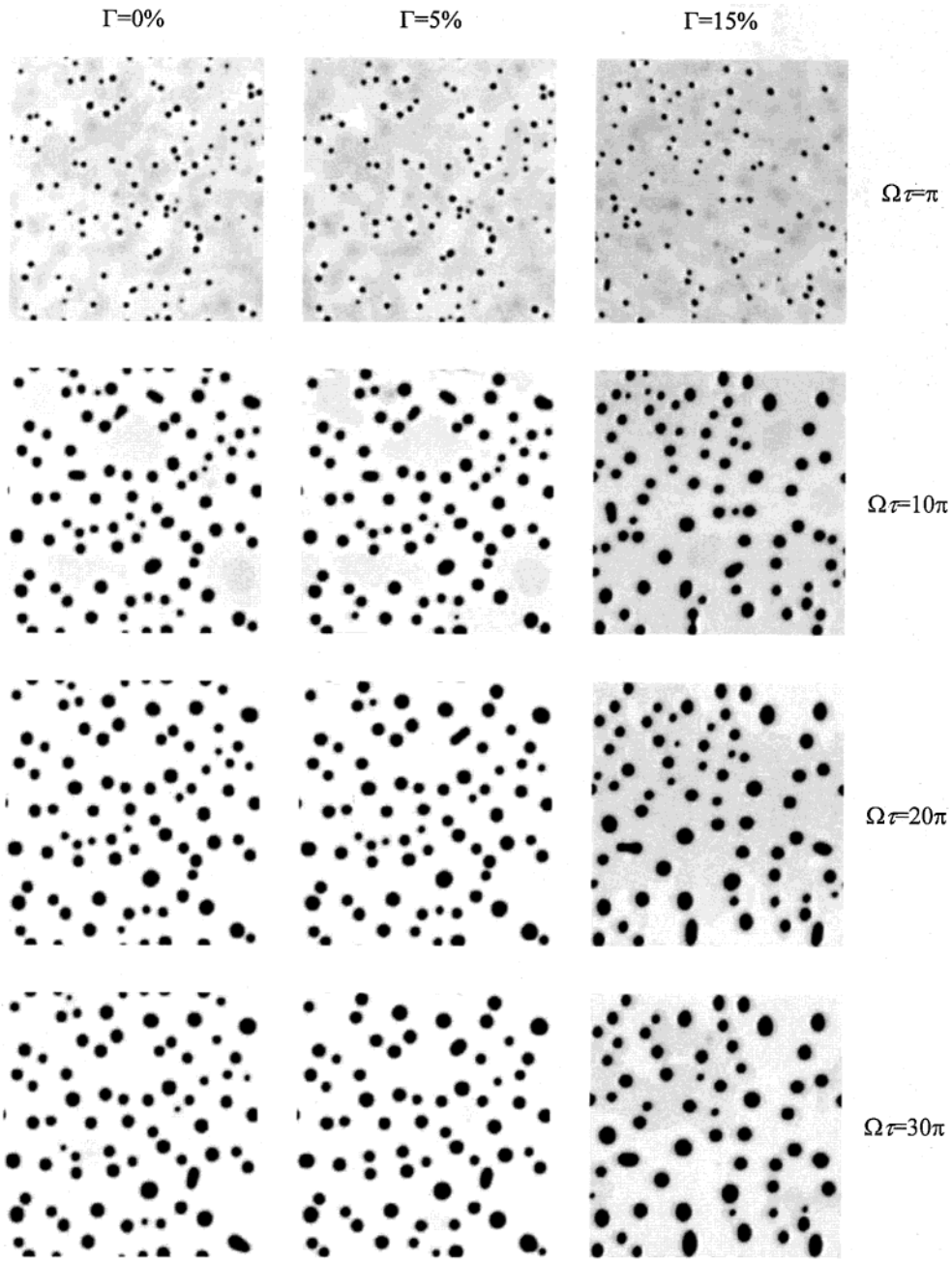

Figure 11. Effect of strain amplitude on the morphology evolution of a 15/85 blend ($A = 1.3$, $\Omega = 0.01$).

introduced the dependence of molecular mobility on composition. To guarantee the numerical stability, the parameter α was set to be 0.6 for composition 20/80 and 1.0 for composition 40/60, respectively. The results are shown in Figures 5 and 6. Although we did not consider the time−temperature shift factor, these figures still show qualitatively the dependence of the moduli on quench depth: the increase of concentration fluctuations leads to an increase in stress. The changes of G' are more obvious than those of G'', due to the fact that the stress induced by the concentration fluctuation is mostly of elastic origin.

From this section, it can be concluded that, under conditions presented here, the quench depth mainly governs the time scale of the phase-separation process and not the kind of morphology that is generated under quiescent conditions. Therefore, a value of 1.3 for A was used throughout the following sections.

The Effects of Shear Amplitude and Frequency on Phase Separation under Oscillatory Flow: Droplet Size Distribution. In the Introduction, we have mentioned that applying an oscillatory shear at low frequency will not affect the critical point of phase separation. However, it might accelerate the coagulation or growth of the phase domains. Experimental[29] or simulation[30,31] studies on this topic are scarce, and they are all dealing with the effect of oscillatory shear on spinodal decomposition. Therefore, we have investigated here the droplet phase separation (20/80) under oscillatory shear with different shear amplitudes and frequencies. In all simulations, A was 1.3, a value which corresponds to a deep quench. The simulated morphology evolution is illustrated in Figure 7. It can be noticed in these images that even an oscillatory shear at a very low frequency ($\Omega = 0.0005$) can accelerate coagulation and growth of the droplet domains, at least under the

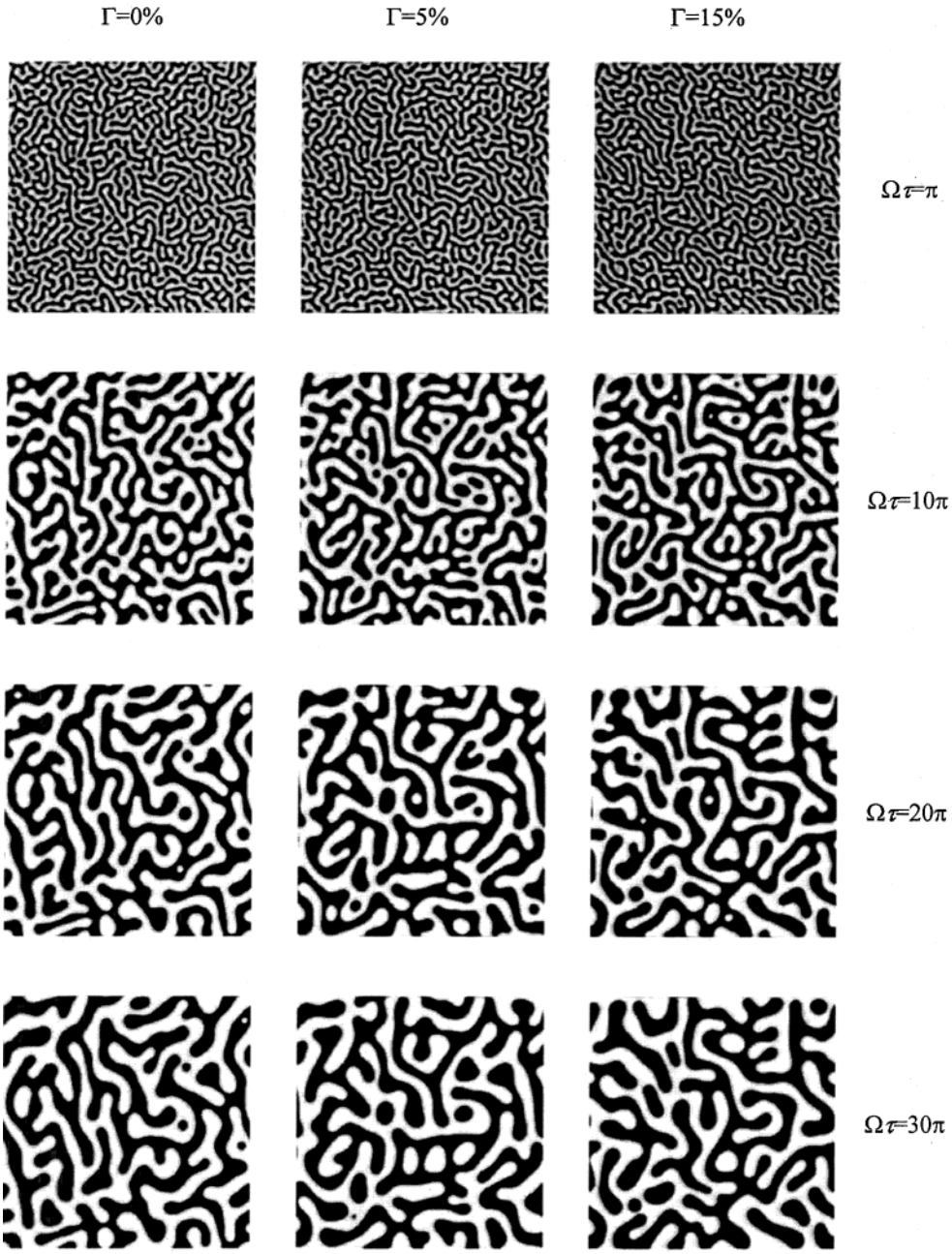

Figure 12. Effect of strain amplitude on the morphology evolution of a 50/50 blend ($A = 1.3$, $\Omega = 0.01$).

investigated amplitudes of 10% and 20%. A higher shear frequency ($\Omega = 0.001$) has a similar effect.

Figure 8, parts a−d, illustrates the corresponding droplet size distributions. It can be seen that the droplet size distribution clearly broadens during the phase-separation process, this broadening becoming more pronounced with increasing shear amplitude. The time evolution of the number and volume average diameter is displayed in Figure 9. It is obvious that both average diameters increase with time, this increase being faster for larger shear amplitudes. The volume-average diameter is more sensitive to the morphology evolution than the number-average diameter.

These findings have been compared to experimental results on a 15/85 PMMA/PαMSAN blend. The blend was allowed to phase separate under quiescent conditions for a well-defined period of time, and subsequently, an oscillatory shear was applied before the sample was quenched for microscopic investigation. During the oscillatory shear the strain amplitude was kept constant ($\Gamma = 0.20$) and the frequency was varied from 100 to 0.01 rad/s (frequency sweep). The resulting droplet size distributions, as seen on the TEM micrographs, are shown in Figure 10, parts a−c. A droplet growth due to phase separation can be observed, as well as a broadening of the size distribution. This is qualitatively consistent with the simulation results.

The Effects of Shear Amplitude and Frequency on Phase Separation under Oscillatory Flow: Rheological Response. As is shown in the previous section, oscillatory flow can affect the morphology formed by phase separation. Under such conditions, the dynamic measurements are no longer a nondestructive morphology probing technique. In the present section, it will be verified whether there still exists a range of low strain amplitudes, frequencies, or composition for which linear (=nondestructive) dynamic measurements are possible. Simulations were performed for a blend in which a

droplet−matrix structure develops (15/85) and one in which a co-continuous morphology is formed (50/50). Experimental results on, respectively, a 15/85 and a 40/60 PMMA/PαMSAN are presented for comparison.

The simulated morphology evolution under oscillatory shear at a relatively high frequency of 0.01 and different shear amplitudes is illustrated in Figures 11 and 12 for the 15/85 and the 50/50 compositions, respectively. In contrast to the previous results for a 20/80 blend (Figure 7), Figure 11 shows almost no difference in morphology evolution for a 15/85 blend under different shear amplitudes. Apparently, the volume fraction of disperse droplets plays a crucial role: 20% is above the percolation limit for a spherical morphology and 15% is slightly below. Consequently, in the former system (oscillatory), flow-induced coalescence will be much easier than in the latter. For a bicontinuous system (50/50), the morphology difference under different shear amplitudes is still very limited, just like for the 15/85 blend. This system will be discussed later.

Figure 13a illustrates the evolution of the storage modulus as a function of time, resulting from the simulations for the 15/85 blend. As mentioned before, the storage modulus is given in a dimensionless form (see section on theory). The time axis represents the period in which phase separation occurred (under quiescent conditions i.e., $\Gamma = 0\%$ or under oscillatory shear with an amplitude of 5 or 15%, respectively); the storage modulus that is plotted is always measured by setting the reduced frequency $\Omega = 0.01$ and the shear amplitude $\Gamma = 5\%$. During nucleation and growth process, molecules will diffuse from the continuous phase to the droplet phase (nuclei). The droplets grow slowly because the diffusion of chains is rather slow. Nevertheless this droplet growth in combination with the increase in volume fraction of disperse phase is responsible for an increase in G'. Subsequently, droplets could coalesce, but this is an even slower process due to the highly viscous matrix and the low fraction of disperse phase. The shear flow only results in slight deformation of droplets as long as the shear amplitude remains limited (<5%). It can be seen in Figure 13a that the rheological response is indeed the same with or without shear during the phase separation period, as long as the strain amplitude during the phase-separation process is below 5% in the present case. A shear amplitude of 15% leads to a higher value of the modulus, even though the differences in the underlying structure of the blend are minor (see Figure 11).

Figure 13b shows the corresponding experimental result of the storage modulus as a function of time. It should be taken into account that the experimental value of the modulus contains—apart from the interfacial contribution—also a contribution from bulk properties of component polymers (eq 9). Nevertheless, for qualitative comparison the curves in Figure 13b can be used as such, because the component contribution is the same constant value throughout all experiments. The agreement between experiment and simulation is quite obvious: in both cases, an increase in storage modulus is observed, which becomes more pronounced for strain amplitudes above a critical value.

In bicontinuous phase separation, a sudden growth of concentration fluctuations creates a highly interconnected structure. This process causes an increase in elasticity of the material (see Figure 4). Because this initial increase in G' is not picked up by the present

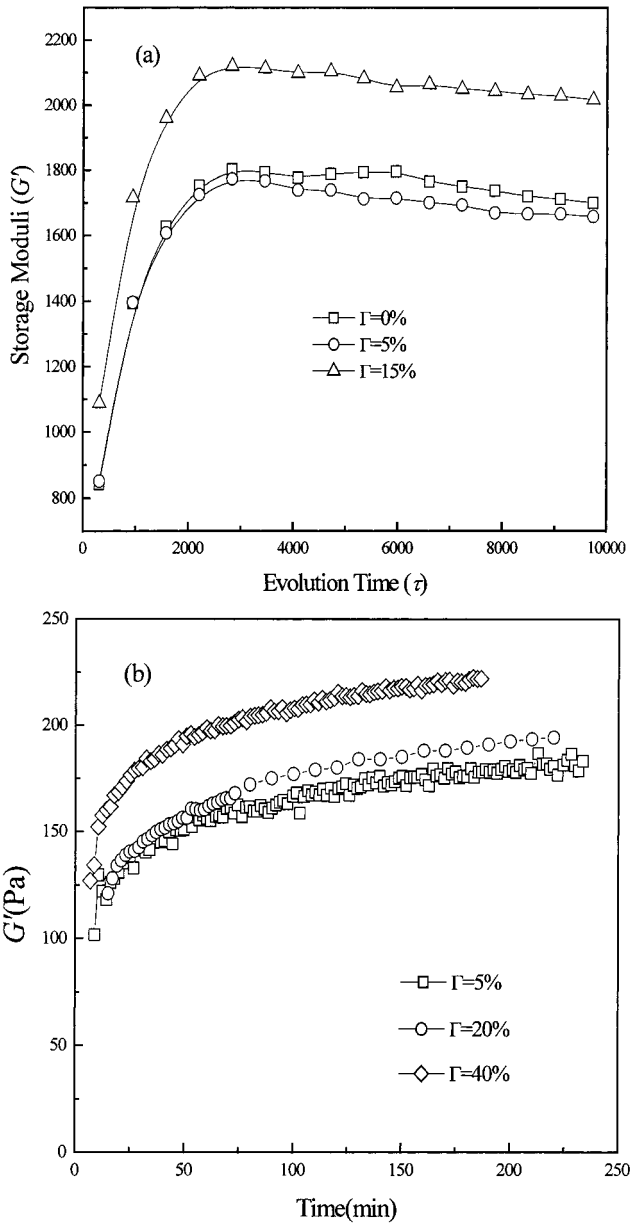

Figure 13. Effect of shear amplitude on storage moduli of phase-separating polymer blends under oscillatory flow: (a) simulation results ($\Omega = 0.01$, $A = 1.3$, composition 15/85); (b) experimental results (15/85 PMMA/PαMSAN at 220 °C).

experiments (Figure 14b), we will focus in this section on the decrease of the storage modulus during the late stage of phase separation. The co-continuous morphology will coarsen during this stage, driven by interfacial tension, and this coarsening process leads to a decreasing storage modulus. The simulations in Figure 14a show that small amplitude oscillations can induce a slightly more pronounced decrease of G' compared to quiescent conditions. This observation agrees with the experimental results (Figure 14b) for the 40/60 PMMA/PαMSAN blend. A plausible explanation is that, for bicontinuous phase separation, the oscillatory shear can accelerate the coagulation of the domains and the breakup of the network strands although the morphology changes are not clear in Figure 12. Both processes lead to a decrease in the degree of co-continuity, the specific interfacial area will be reduced and the stress contribution of the interface decreases.

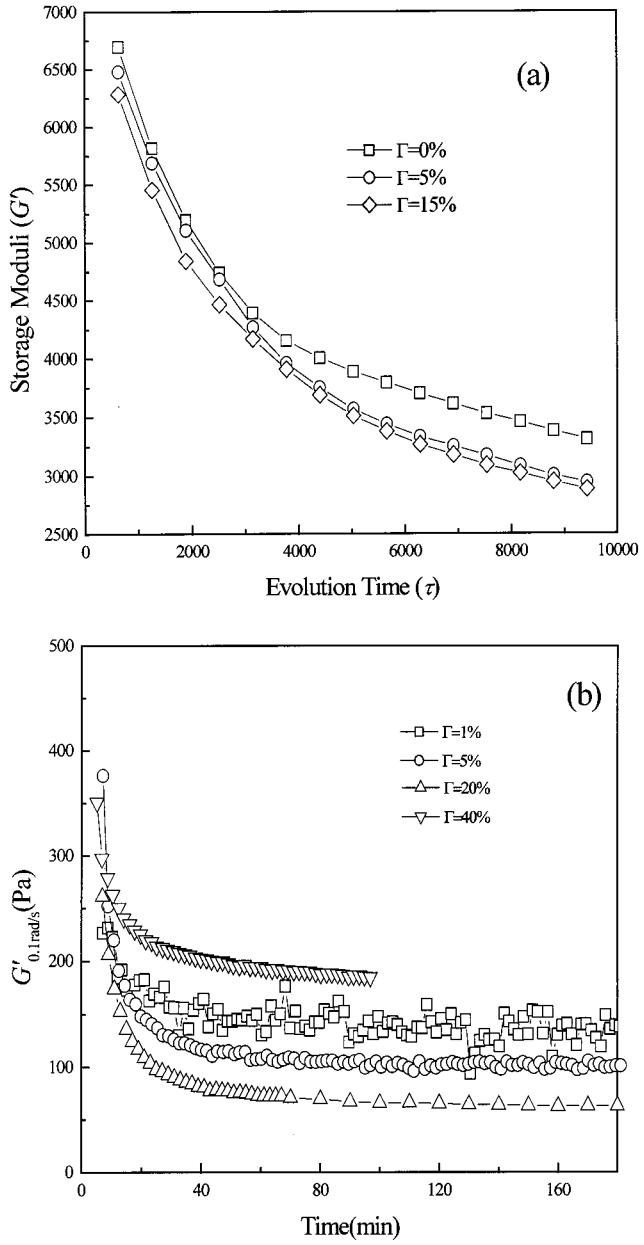

Figure 14. Effect of shear amplitude on storage moduli of phase-separating polymer blends under oscillatory flow (a) simulation results ($\Omega = 0.01$, $A = 1.3$, composition 50/50); (b) experimental results (50/50 PMMA/PαMSAN at 220 °C).

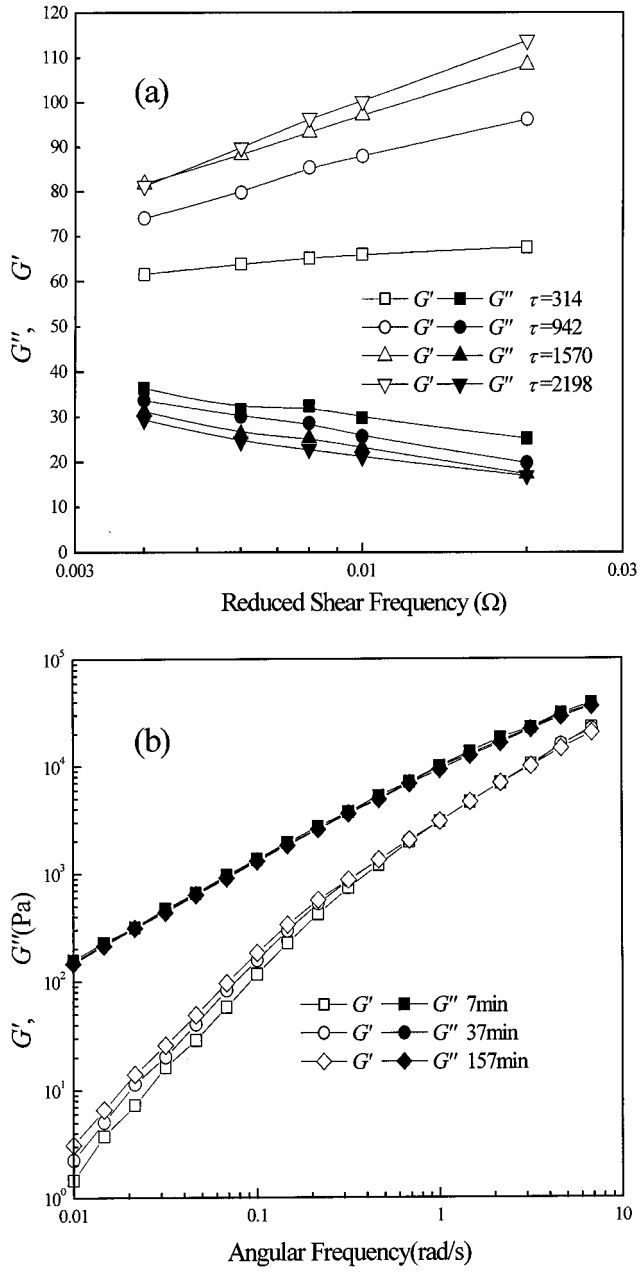

Figure 15. (a) Simulation results of frequency sweep of phase-separating polymer blend (composition 15/85, $\Gamma = 5\%$). (b) Dynamic spectrum of 15/85 PMMA/PαMSAN, measured after a well-defined period (7−37−157 min) of phase separation under quiescent conditions at 220 °C. The shear amplitude was 20%.

Actually a rather complex picture is observed in the experimental results. When the shear amplitude exceeds 20%, an increase in amplitude results in a less pronounced decay of G'. It should be mentioned that in the present simulations a shear amplitude above 15% could not be applied due to numerical instabilities. Nevertheless, it can be noticed that the difference between the simulated results for 5% and 15% strain is much less than that for 0% and 5%. A possible explanation for this observation is given by Krall et al.,[41] based on numerical solution the model of Doi and Ohta.[41] For large values of strain amplitude the distortion is effective enough to stop the domain growth, resulting in a dynamic equilibrium of the domain size distribution. In this case, the steady-state value of the elastic modulus is a decreasing function of strain. For small values of strain amplitude, the effect of shear becomes weak and domain growth can proceed up to macroscopic phase separation. The storage modulus will decay to zero but the rate at which this happens is strain dependent. When the modulus is calculated after a limited period of phase separation,[41] the complex strain dependence of the storage modulus that was observed in Figure 14b is retrieved.

The time evolution of the simulated dynamic spectrum is displayed in Figures 15a and 16a for blend compositions of, respectively, 15/85 and 50/50. First a period of phase separation under quiescent conditions was simulated, followed by a simulation of the rheological response. For droplet phase separation, an increase in G' in the range of low frequencies is observed; G'' is less sensitive to the morphology evolution. For bicontinuous phase separation, however, a drop in the G' curves is observed in the range of low frequencies. Again, G'' is less sensitive to the structure

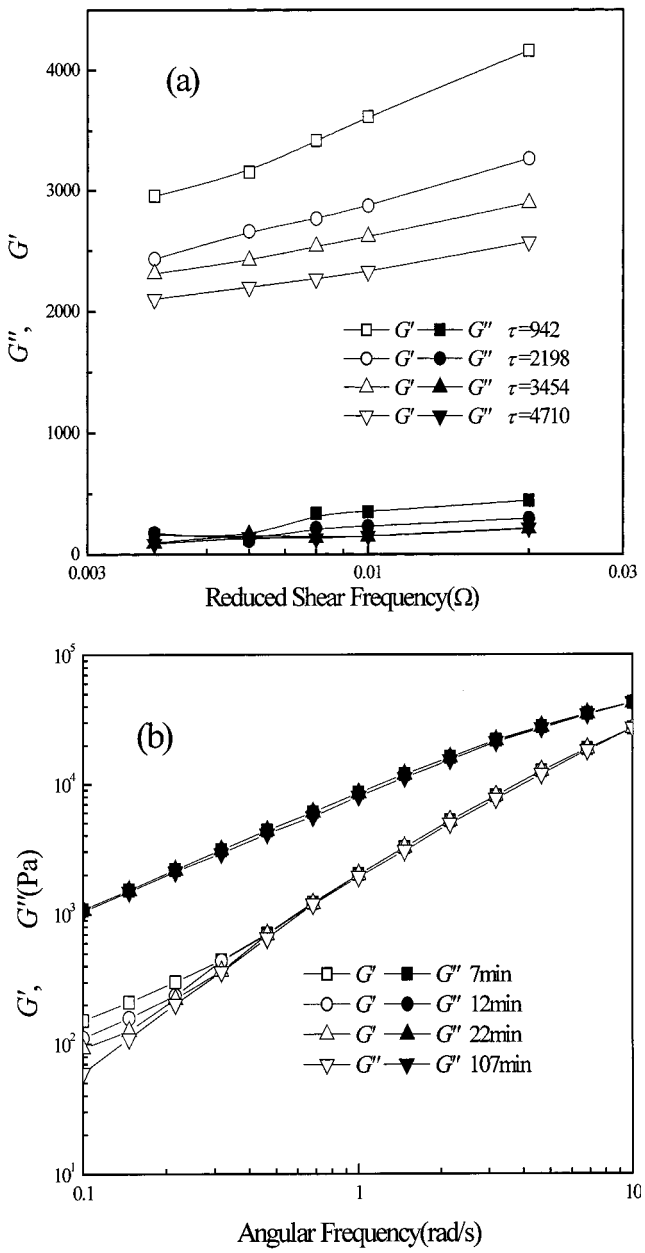

Figure 16. (a) Simulation results of frequency sweep of phase-separating polymer blend (composition 50/50, $\Gamma = 5\%$). (b) Dynamic spectrum of 40/60 PMMA/PαMSAN, measured after a well-defined period (7−12−22−107 min) of phase separation under quiescent conditions at 220 °C. The shear amplitude was 20%.

evolution. This difference in behavior can be explained by the difference in phase separation mechanism, as has been mentioned previously. Figures 15b and 16b show the corresponding experimental results for 15/85 and 40/60 PMMA/PαMSAN. Here, the total stress response is presented, not only the interfacial contribution. Again, simulations and experiments agree: an enhanced elasticity is observed at low frequency for the matrix−droplet system. In contrast to this, a reduced elasticity is observed at low frequency for the bicontinuous system. However, the loss modulus is almost unaffected by the phase-separation process.

V. Conclusions

Systematic simulations of phase separation under oscillatory shear have been presented. Both the morphology evolution and the stress response from the interface have been calculated. For the latter, the expression of Kawasaki[38] has been used. This equation indicates that both the strength of concentration fluctuations and the specific interfacial area determine the stress contribution of interfacial relaxation. Compared with the stress tensor proposed by Fredrickson and Larson[22] and the emulsion model of Palierne,[18] the expression of the stress tensor by Kawasaki is more universal.

The simulations are confronted directly with experimental results on PMMA/PαMSAN blends to evaluate the potential of the such kind of simulations. The effect of different parameters on the morphology evolution and rheology during phase separation has been investigated. An increase in quench depth leads to stronger concentration fluctuations, faster phase separation, and an increased elasticity of the sample. Concerning the effect of an oscillatory shear, a difference between droplet phase separation and bicontinuous phase separation should be made. For droplet phase separation, the growth of domains is determined by an evaporation−condensation mechanism, which is quite slow in a highly viscous matrix. The corresponding storage modulus gradually increases with time. The effect of the oscillatory shear on the morphology formation depends on the composition. For a composition of 20/80, an oscillatory shear—even at very low frequency—can accelerate the coagulation of droplets. However for a composition of 15/85, the effect remains limited provided that the amplitude is small (<5%).

For bicontinuous phase separation, the concentration fluctuations reach their saturation level value very quickly. Subsequently, the domains grow, driven by the interfacial tension. Because of this domain growth the specific interfacial area in the system decreases, resulting in a decrease in stress. Consequently, the simulated G' values decrease with time. The domain growth can be accelerated by shear—even at small amplitudes—and a more pronounced decay of G' can be found. In both cases, G'' is not so sensitive as G'. These findings are in good qualitative agreement with the experimental results.

Acknowledgment. The authors are indebted to Drs. W. Heckmann and T. Frechen (BASF) for providing the micrographs and to G. Schmidt (BASF) for support with the rheological measurements. Inge Vinckier is indebted to the FWO-Vlaanderen for a postdoctoral fellowship. This work was also subsidized by the Special Funds for Major State Basic Research Projects, Ministry of S & T. Partial financial support from NDFC and Shanghai Research and Development Center for Polymeric Materials are also acknowledged.

References and Notes

(1) Prest, W. M.; Porter, R. S. *J. Polym. Sci.* **1972**, *A-2* 10, 1639−1655.
(2) Araujo, M. A.; Stadler, R. *Makromol. Chem.* **1988**, *189*, 2169−2186.
(3) Brekner, M. J.; Cantow, H. J.; Schneider, H. A. *Polym. Bull.* **1985**, *14*, 17−24.
(4) Irving, J. B. In *Viscosities of Binary Liquid Mixtures: A Survey of Mixture Equations*; Report No. 630. National Engineering Laboratory: East Kilbridge, Glasgow, U.K., 1977.
(5) Mertsch, R.; Wolf, B. A. *Ber. Bunsen-Ges. Phys. Chem.* **1994**, *98*, 1275−1280.
(6) Vlassopoulos, D.; Koumoutsakos, A.; Anastasiadis, H.; Hatzikiriakos, S. G.; Englezos, P. *J. Rheol.* **1997**, *41*, 739−755.

(7) Kapnistos, M.; Hinrichs, A.; Vlassopoulos, D.; Anastasiadis, S. H.; Stammer, A.; Wolf, B. A. *Macromolecules* **1996**, *29*, 7155−7163.
(8) Takahashi, Y.; Suzuki, H.; Nakagawa, Y.; Noda, I. *Polym. Int.* **1994**, *34*, 327−331.
(9) Chopra, D.; Vlassopoulos, D.; Hatzikiriakos, S. G. *J. Rheol.* **2000**, *44*, 27−46.
(10) Ajji, A.; Choplin, L.; Prud'homme, R. E. *J. Polym. Sci., Polym. Phys. Ed.* **1991**, *29*, 1573−1578.
(11) Mani, S.; Malone, M. F.; Winter, H. H. *J. Rheol.* **1992**, *36*, 1625−1649.
(12) Polios, I. S.; Soliman, M.; Lee, C.; Gido, S. P.; Schmidt-Rohr, K.; Winter, H. H. *Macromolecules* **1997**, *30*, 4470−4480.
(13) Kapnistos, M.; Vlassopoulos, D.; Anastasiadis, S. H. *Europhys. Lett.* **1996**, *34*, 513−518.
(14) Han, C. D. *Multiphase Flow in Polymer Processing*; Academic: New York, 1981.
(15) Vinckier, I.; Moldenaers, P.; Mewis. J. *J. Rheol.* **1996**, *40*, 613−631.
(16) Graebling, D.; Muller, R. *J. Rheol.* **1990**, *34*, 193−206.
(17) Graebling, D.; Muller, R.; Palierne, J. F. *Macromolecules* **1993**, *26*, 320−329.
(18) Palierne, J. F. *Rheol. Acta* **1990**, *29*, 204−214.
(19) Gramespacher, H.; Meissner, J. *J. Rheol.* **1992**, *36*, 1127−1141.
(20) Friedrich, C.; Gleinser, W.; Korat, E.; Maier, D.; Weese, J. *J. Rheol.* **1995**, *39*, 1411−1425.
(21) Vinckier, I.; Laun, H. M. *Rheol. Acta*, **1999**, *38*, 274−286.
(22) Fredrickson, G. H.; Larson, R. G. *J. Chem. Phys.* **1987**, *86*, 1553−1560.
(23) Hindawi, I.; Higgins, J. S.; Weiss, R. A. *Polymer* **1992**, *33*, 2522−2530.
(24) Katsaros, J. D.; Malone, M. F.; Winter, H. H. *Polym. Eng. Sci.* **1989**, *29*, 1434−1445.
(25) Fernandez, M. L.; Higgins, J. S.; Horst, R.; Wolf, B. A. *Polymer* **1995**, *36*, 149−154.
(26) Larson, R. G. *Rheol. Acta* **1992**, *31*, 497−520.
(27) Horst, R.; Wolf, B. A. *Macromolecules* **1993**, *26*, 5676−5680.
(28) Onuki, A. *J. Phys.: Condens. Matter*. **1997**, *9*, 6119−6157.
(29) Matsuzaka, K.; Jinnai, H.; Koga, T.; Hashimoto, T. *Macromolecules* **1997**, *30*, 1146−1152.
(30) Qiu, F.; Zhang, H. D.; Yang, Y. L. *J. Chem. Phys.* **1998**, *109*, 1575−1583.
(31) (a) Qiu, F.; Zhang, H. D.; Yang, Y. L. *J. Chem. Phys.* **1998**, *108*, 9529−9535. (b) Zhang, Z. L.; Zhang, H. D.; Yang, Y. L. *J. Chem. Phys.* **2000**, in press.
(32) de Gennes, P. G. *J. Chem. Phys.* **1980**, *72*, 4756.
(33) Ohta, T.; Nosaki, H.; Doi, M. *J. Chem. Phys.* **1990**, *93*, 2664−2675.
(34) Onoo, Y.; Puri, S. *Phys. Rev. Lett.* **1987**, *58*, 836.
(35) Onoo, Y.; Puri, S. *Phys. Rev. A* **1988**, *38*, 434.
(36) Roths, T.; Maier, D.; Friedrich, C.; Honerkamp, J. *Proceedings of the 15th PPS Meeting*, 's Hertogenbosch; The Netherlands, 1999.
(37) Ohta, T.; Enomoto, Y.; Harden, J. L.; Doi, M. *Macromolecules* **1993**, *26*, 4928.
(38) Kawasaki, K.; Ohta, T. *Physica A* **1986**, *139*, 223.
(39) Laun, H. M. *Pure Appl. Chem.* **1998**, *70*, 1547−1566.
(40) Takeno, H.; Hashimoto, T. *J. Chem. Phys* **1998**, *108*, 1225−1233.
(41) Krall, A. H.; Sengers, J. V.; Hamano, K. *Phys. Rev. E* **1993**, *48*, 357−376.
(42) Doi, M.; Ohta, T. *J. Chem. Phys.* **1991**, *95*, 1242−1248.

MA000968F